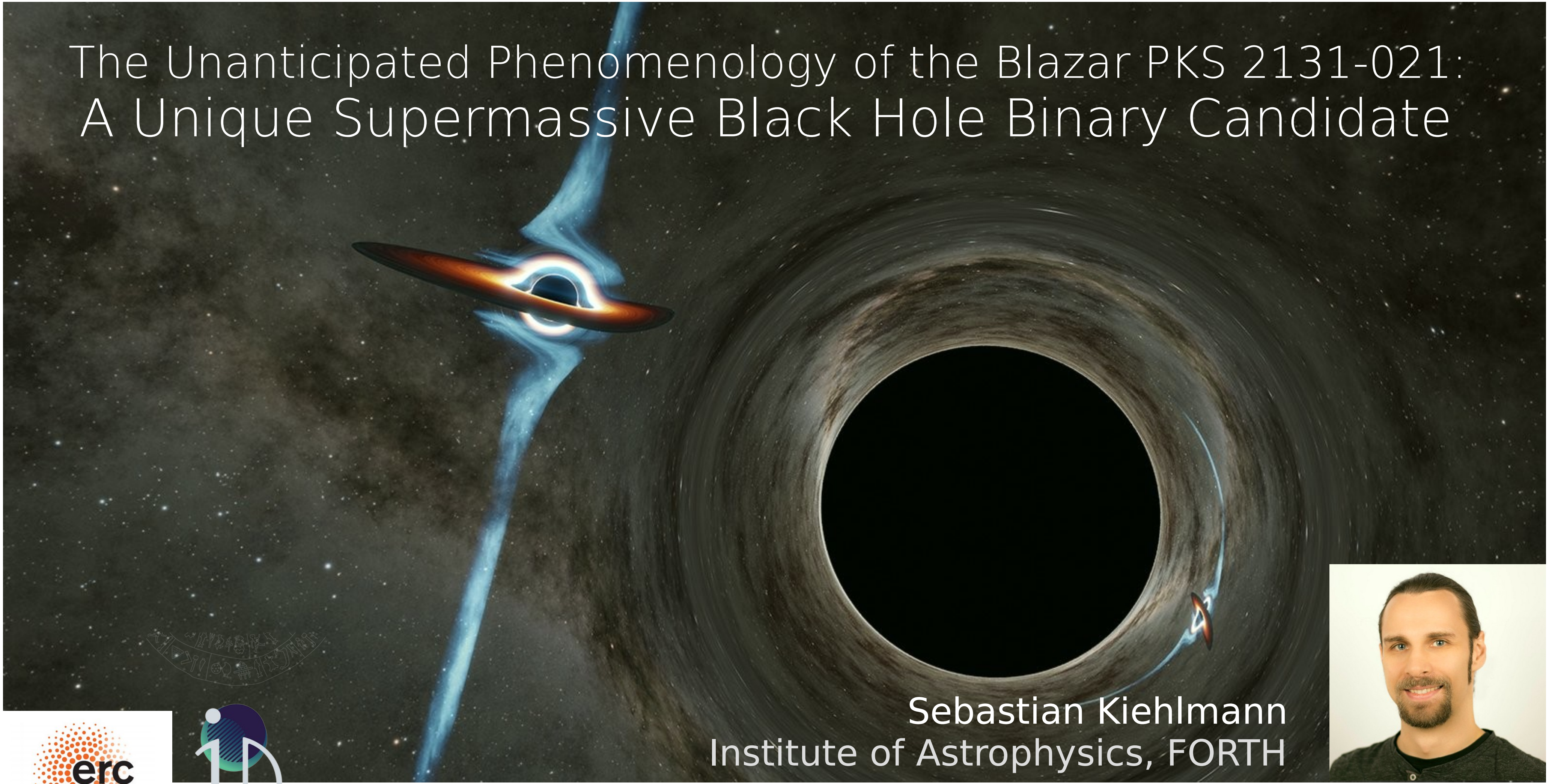

The Unanticipated Phenomenology of the Blazar PKS 2131-021: A Unique Supermassive Black Hole Binary Candidate

Sebastian Kiehlmann
Institute of Astrophysics, FORTH

European Research Council
Established by the European Commission

Synopsis

- 45 years radio light curve of PKS 2131-021
  - two epochs of strong sinusoidal variation with the same period and phase
    - unlikely due to random fluctuations at 4.6σ significance level
      - suggests a Super Massive Black Hole Binary (SMBHB)

45 years radio light curve: two epochs of periodic signal

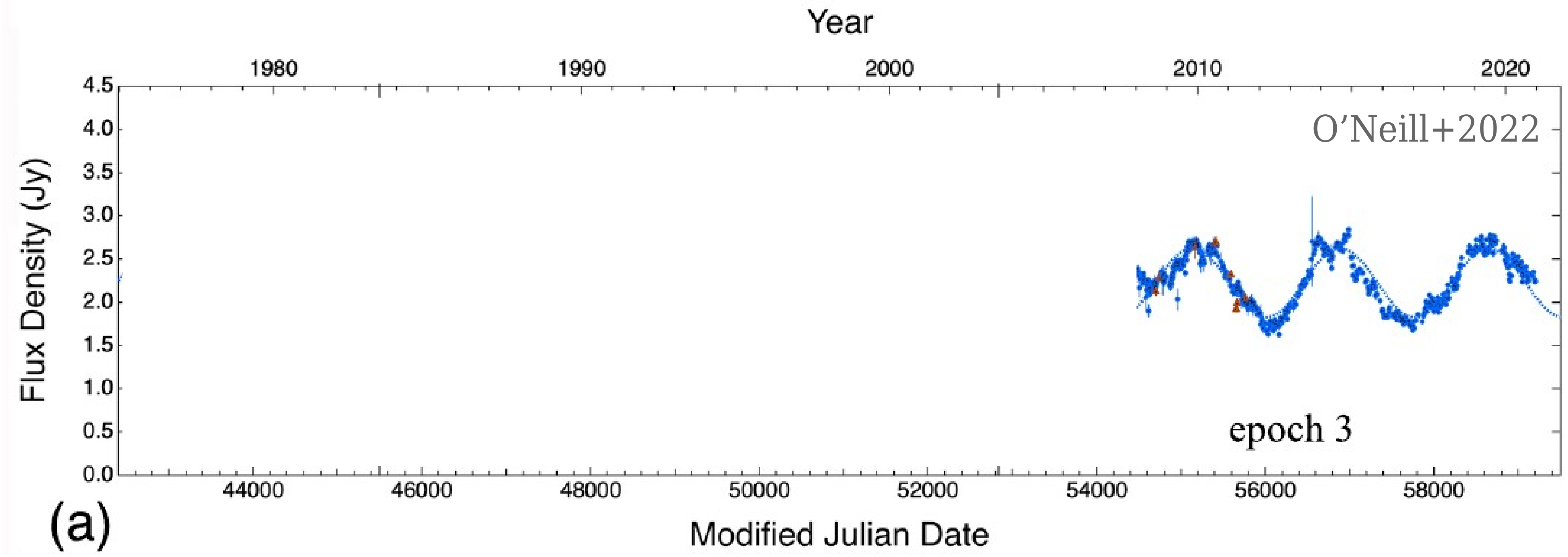

45 years radio light curve: two epochs of periodic signal

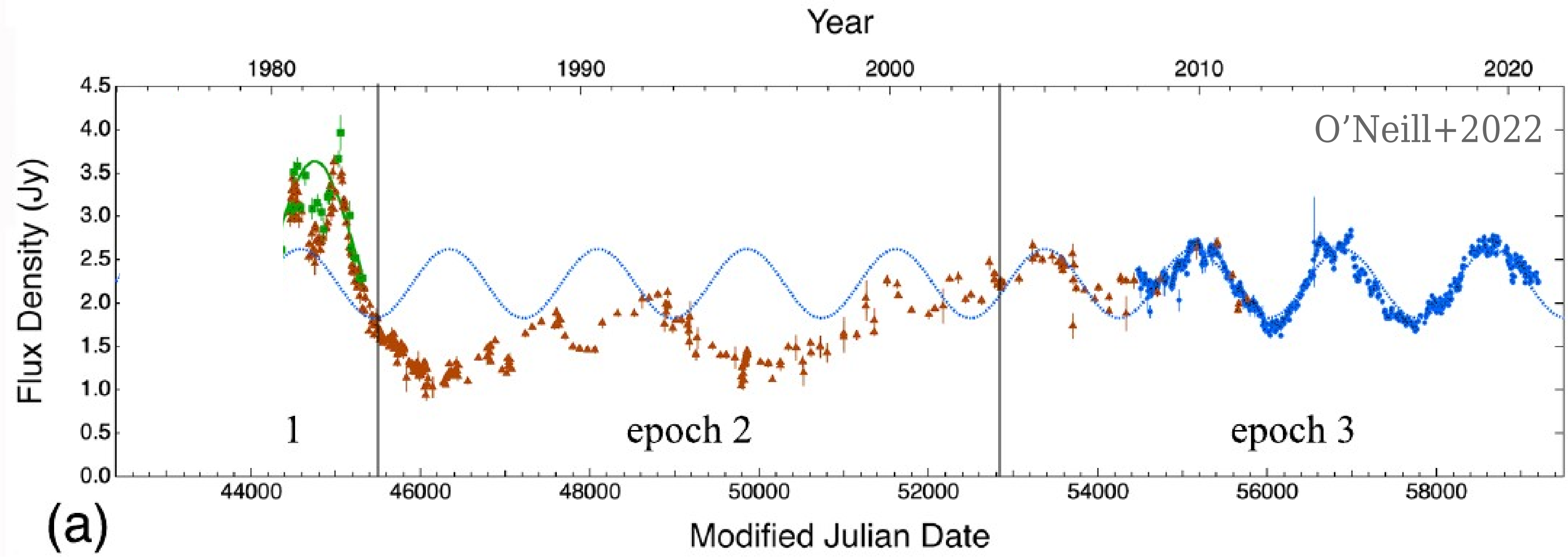

45 years radio light curve: two epochs of periodic signal

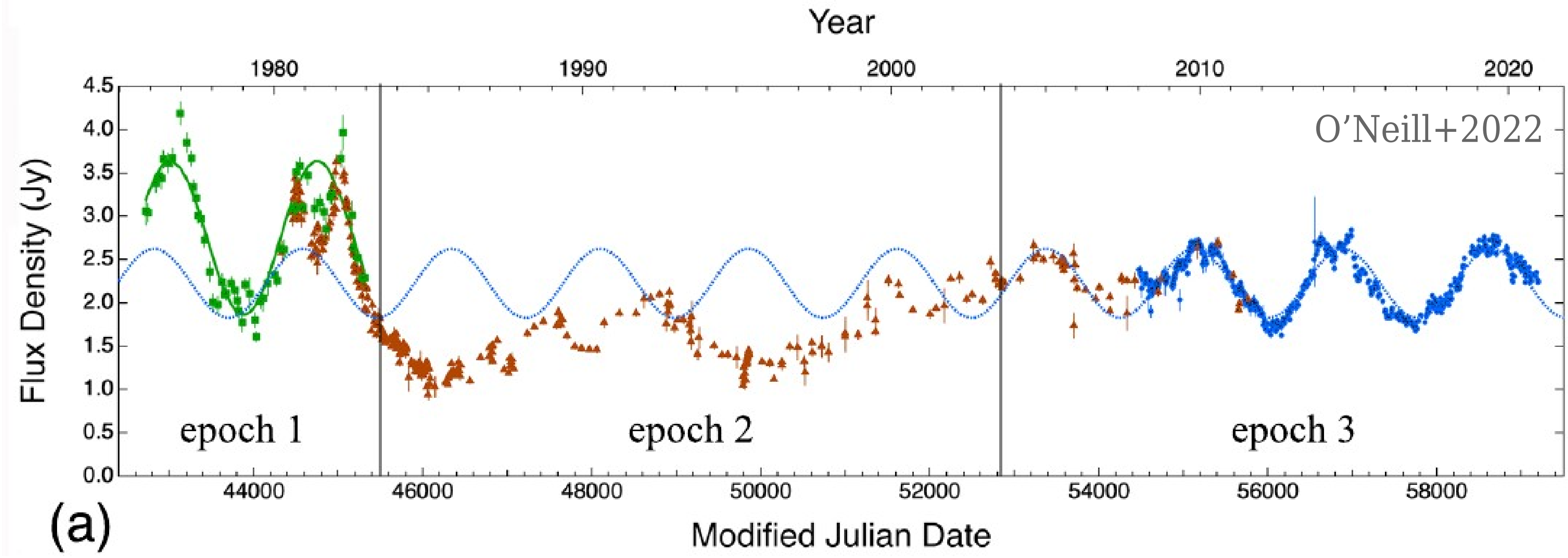

Sinusoid fits: two epochs with matching period and phase

Table 1
Sine-fitting Results for Epoch 1, Epoch 2, Epoch 3, and the Joint Epoch 1 + Epoch 3 Data Sets

	epoch 1	epoch 2	epoch 3	epoch 1 + epoch 3
P (days)	1729.1 ± 32.4	3779.1 ± 46.0	1760.4 ± 5.3	1737.9 ± 2.6
ϕ_0	0.89 ± 0.46	0.35 ± 0.08	0.60 ± 0.07	0.88 ± 0.03
A (epoch 1)	0.709 ± 0.047	...	...	0.679 ± 0.045
S_0 (epoch 1)	2.553 ± 0.036	...	...	2.584 ± 0.034
σ_0 (epoch 1)	0.333 ± 0.022	...	...	0.337 ± 0.023
A (epoch 2)	...	0.392 ± 0.020	...	...
S_0 (epoch 2)	...	1.724 ± 0.021	...	...
σ_0 (epoch 2)	...	0.140 ± 0.009	...	...
A (epoch 3)	...	...	0.400 ± 0.007	0.400 ± 0.007
S_0 (epoch 3)	...	...	2.225 ± 0.005	2.229 ± 0.005
σ_0 (epoch 3)	...	...	0.118 ± 0.004	0.120 ± 0.004

Note. We also determined the least-squares sine fit to epoch 3 for shifted boundaries between epoch 2 and epoch 3 at MJD 51,200 and MJD 53,800, with the results $P = 1762.9 \pm 6.1$ days and $P = 1756.0 \pm 5.5$ days, respectively. These may be compared with the result above of $P = 1760.4 \pm 5.3$ days for the boundary set at MJD 52,850. The peak periods identified in our WWZ analyses of epochs 1, 2, and 3 were 1740, 3919, and 1779 days, respectively. Those in our GLS analyses were 1730, 3937, and 1788 days, respectively.

O'Neill+2022

Sinusoid fits: two epochs with matching period and phase

Table 1
Sine-fitting Results for Epoch 1, Epoch 2, Epoch 3, and the Joint Epoch 1 + Epoch 3 Data Sets

	epoch 1	epoch 2	epoch 3	epoch 1 + epoch 3
P (days)	1729.1 ± 32.4	3779.1 ± 46.0	1760.4 ± 5.3	1737.9 ± 2.6
ϕ_0	0.89 ± 0.46	0.35 ± 0.08	0.60 ± 0.07	0.88 ± 0.03
A (epoch 1)	0.709 ± 0.047	...	...	0.679 ± 0.045
S_0 (epoch 1)	2.553 ± 0.036	...	...	2.584 ± 0.034
σ_0 (epoch 1)	0.333 ± 0.022	...	...	0.337 ± 0.023
A (epoch 2)	...	0.392 ± 0.020	...	...
S_0 (epoch 2)	...	1.724 ± 0.021	...	...
σ_0 (epoch 2)	...	0.140 ± 0.009	...	...
A (epoch 3)	...	...	0.400 ± 0.007	0.400 ± 0.007
S_0 (epoch 3)	...	...	2.225 ± 0.005	2.229 ± 0.005
σ_0 (epoch 3)	...	...	0.118 ± 0.004	0.120 ± 0.004

Note. We also determined the least-squares sine fit to epoch 3 for shifted boundaries between epoch 2 and epoch 3 at MJD 51,200 and MJD 53,800, with the results $P = 1762.9 \pm 6.1$ days and $P = 1756.0 \pm 5.5$ days, respectively. These may be compared with the result above of $P = 1760.4 \pm 5.3$ days for the boundary set at MJD 52,850. The peak periods identified in our WWZ analyses of epochs 1, 2, and 3 were 1740, 3919, and 1779 days, respectively. Those in our GLS analyses were 1730, 3937, and 1788 days, respectively.

O'Neill+2022

Sinusoid fits: two epochs with matching period and phase

Table 1
Sine-fitting Results for Epoch 1, Epoch 2, Epoch 3, and the Joint Epoch 1 + Epoch 3 Data Sets

	epoch 1	epoch 2	epoch 3	epoch 1 + epoch 3
P (days)	1729.1 ± 32.4	3779.1 ± 46.0	1760.4 ± 5.3	1737.9 ± 2.6
ϕ_0	0.89 ± 0.46	0.35 ± 0.08	0.60 ± 0.07	0.88 ± 0.03
A (epoch 1)	0.709 ± 0.047	...	...	0.679 ± 0.045
S_0 (epoch 1)	2.553 ± 0.036	...	...	2.584 ± 0.034
σ_0 (epoch 1)	0.333 ± 0.022	...	...	0.337 ± 0.023
A (epoch 2)	...	0.392 ± 0.020	...	...
S_0 (epoch 2)	...	1.724 ± 0.021	...	...
σ_0 (epoch 2)	...	0.140 ± 0.009	...	...
A (epoch 3)	...	...	0.400 ± 0.007	0.400 ± 0.007
S_0 (epoch 3)	...	...	2.225 ± 0.005	2.229 ± 0.005
σ_0 (epoch 3)	...	...	0.118 ± 0.004	0.120 ± 0.004

Note. We also determined the least-squares sine fit to epoch 3 for shifted boundaries between epoch 2 and epoch 3 at MJD 51,200 and MJD 53,800, with the results $P = 1762.9 \pm 6.1$ days and $P = 1756.0 \pm 5.5$ days, respectively. These may be compared with the result above of $P = 1760.4 \pm 5.3$ days for the boundary set at MJD 52,850. The peak periods identified in our WWZ analyses of epochs 1, 2, and 3 were 1740, 3919, and 1779 days, respectively. Those in our GLS analyses were 1730, 3937, and 1788 days, respectively.

O'Neill+2022

Generalized Lomb-Scargle Periodogram

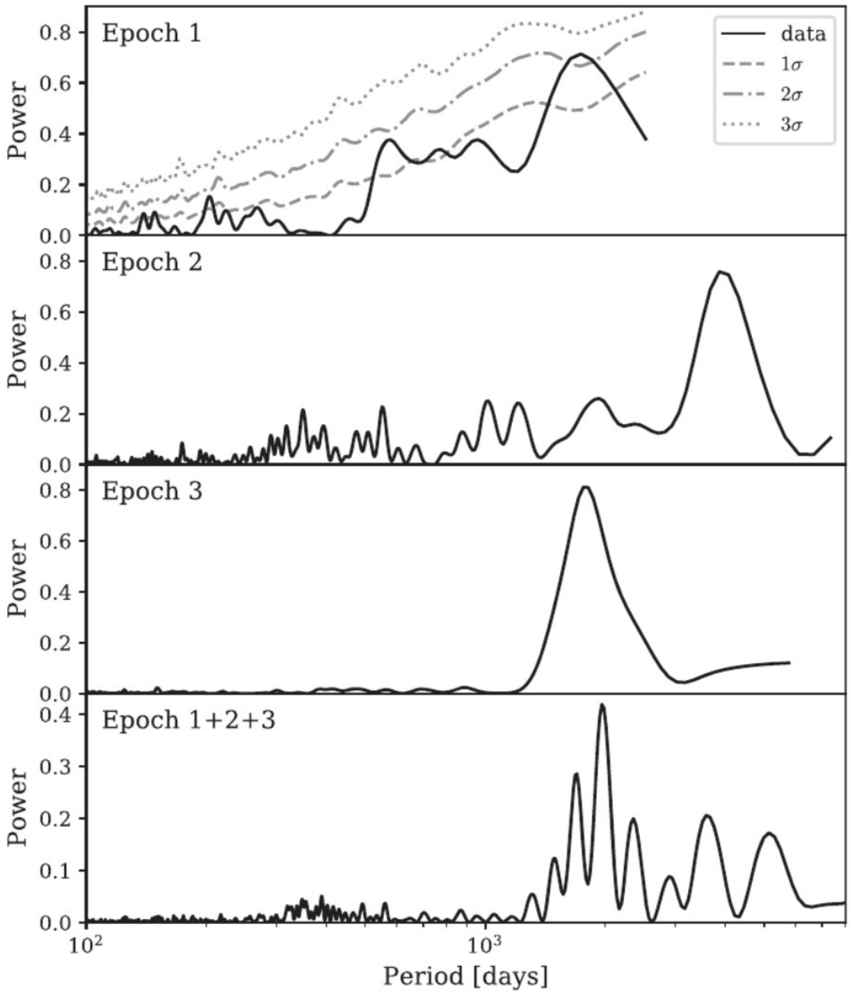

O'Neill+2022

Generalized Lomb-Scargle Periodogram: significance

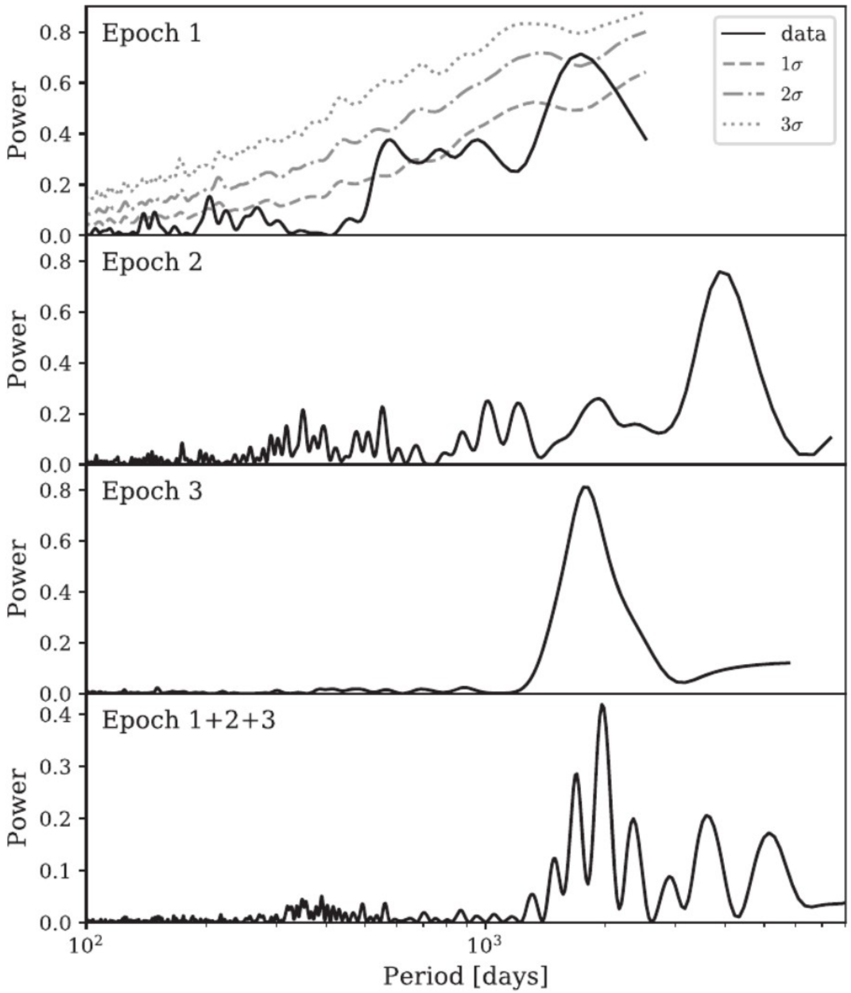

O'Neill+2022

H0: variability follows a red noise process (i.e. is purely stochastic)

H1: variability has a periodic component

Table 3
Single-period (Spurious) and All-period (True) Probabilities

Epoch and Test	N_{tot}	n_{pass}	p-value	σ
epoch 1 single period	10000	108	1.08×10^{-2}	2.3
epoch 1 all periods	10000	1446	1.45×10^{-1}	1.06[a]
epoch 2 single period	10000	122	2.20×10^{-3}	2.85
epoch 2 all periods	10000	632	6.32×10^{-2}	1.53[a]
epoch 3 single period	100000	0	$<10^{-5}$	$>$4.26
epoch 3 all periods	100000	40	4.00×10^{-4}	3.35[a]

Note. The tests using all periods are the "Look Elsewhere" tests.
[a] These are the true significances; the others are totally spurious unless the periods have been selected "a priori."

O'Neill+2022

A highly significant detection

Table 2
Probabilities and Significance Levels of GLS Tests Computed from Simulations with Matched Red-noise Tail

Test Number	Test	GLS $\mathcal{P}_{peak}$ (max = 1)	Period Range (ΔP) (days)	Total Simulations	Number of Simulations That Pass Test	p-value	Significance (σ)
1.1	epoch 1 $\mathcal{P}_{peak}$, $p_{sim} \leqslant p_{peak}$	0.71	All	10,000	1446	1.45×10^{-1}	1.06
1.2	epoch 2 $\mathcal{P}_{peak}$, $p_{sim} \leqslant p_{peak}$	0.76	All	10,000	632	6.32×10^{-2}	1.53
1.3	epoch 3 $\mathcal{P}_{peak}$, $p_{sim} \leqslant p_{peak}$	0.81	All	100,000	40	4.0×10^{-4}	3.35
2	epoch 1 $\mathcal{P}_{lim}$, $\Delta P_{epoch\ 3}$	$\geqslant$0.50	1661.9–1858.9	10,000	197	1.97×10^{-2}	2.06
3	1.3+2	…	…	…	…	7.88×10^{-6}	4.32
4	3+phase	…	…	…	…	1.58×10^{-6}	4.66

O’Neill+2022

A highly significant detection

Table 2
Probabilities and Significance Levels of GLS Tests Computed from Simulations with Matched Red-noise Tail

Test Number	Test	GLS $\mathcal{P}_{\rm peak}$ (max = 1)	Period Range (ΔP) (days)	Total Simulations	Number of Simulations That Pass Test	p-value	Significance (σ)
1.1	epoch 1 $\mathcal{P}_{\rm peak}$, $p_{\rm sim} \leqslant p_{\rm peak}$	0.71	All	10,000	1446	1.45×10^{-1}	1.06
1.2	epoch 2 $\mathcal{P}_{\rm peak}$, $p_{\rm sim} \leqslant p_{\rm peak}$	0.76	All	10,000	632	6.32×10^{-2}	1.53
1.3	epoch 3 $\mathcal{P}_{\rm peak}$, $p_{\rm sim} \leqslant p_{\rm peak}$	0.81	All	100,000	40	4.0×10^{-4}	3.35
2	epoch 1 $\mathcal{P}_{\rm lim}$, $\Delta P_{\rm epoch\ 3}$	$\geqslant$0.50	1661.9–1858.9	10,000	197	1.97×10^{-2}	2.06
3	1.3+2	…	…	…	…	7.88×10^{-6}	4.32
4	3+phase	…	…	…	…	1.58×10^{-6}	4.66

O’Neill+2022

A highly significant detection

Table 2
Probabilities and Significance Levels of GLS Tests Computed from Simulations with Matched Red-noise Tail

Test Number	Test	GLS $\mathcal{P}_{\rm peak}$ (max = 1)	Period Range (ΔP) (days)	Total Simulations	Number of Simulations That Pass Test	p-value	Significance (σ)
1.1	epoch 1 $\mathcal{P}_{\rm peak}$, $p_{\rm sim} \leqslant p_{\rm peak}$	0.71	All	10,000	1446	1.45×10^{-1}	1.06
1.2	epoch 2 $\mathcal{P}_{\rm peak}$, $p_{\rm sim} \leqslant p_{\rm peak}$	0.76	All	10,000	632	6.32×10^{-2}	1.53
1.3	epoch 3 $\mathcal{P}_{\rm peak}$, $p_{\rm sim} \leqslant p_{\rm peak}$	0.81	All	100,000	40	4.0×10^{-4}	3.35
2	epoch 1 $\mathcal{P}_{\rm lim}$, $\Delta P_{\rm epoch\ 3}$	$\geqslant$0.50	1661.9–1858.9	10,000	197	1.97×10^{-2}	2.06
3	1.3+2	⋯	⋯	⋯	⋯	7.88×10^{-6}	4.32
4	3+phase	⋯	⋯	⋯	⋯	1.58×10^{-6}	4.66

O’Neill+2022

A highly significant detection

Table 2
Probabilities and Significance Levels of GLS Tests Computed from Simulations with Matched Red-noise Tail

Test Number	Test	GLS $\mathcal{P}_{peak}$ (max = 1)	Period Range (ΔP) (days)	Total Simulations	Number of Simulations That Pass Test	p-value	Significance (σ)
1.1	epoch 1 $\mathcal{P}_{peak}$, $p_{sim} \leqslant p_{peak}$	0.71	All	10,000	1446	1.45×10^{-1}	1.06
1.2	epoch 2 $\mathcal{P}_{peak}$, $p_{sim} \leqslant p_{peak}$	0.76	All	10,000	632	6.32×10^{-2}	1.53
1.3	epoch 3 $\mathcal{P}_{peak}$, $p_{sim} \leqslant p_{peak}$	0.81	All	100,000	40	4.0×10^{-4}	3.35
2	epoch 1 $\mathcal{P}_{lim}$, $\Delta P_{epoch\ 3}$	$\geqslant$0.50	1661.9–1858.9	10,000	197	1.97×10^{-2}	2.06
3	1.3+2	...	...	...	...	7.88×10^{-6}	4.32
4	3+phase	...	...	...	...	1.58×10^{-6}	4.66

O'Neill+2022

Model: Doppler boosting in black hole binary system

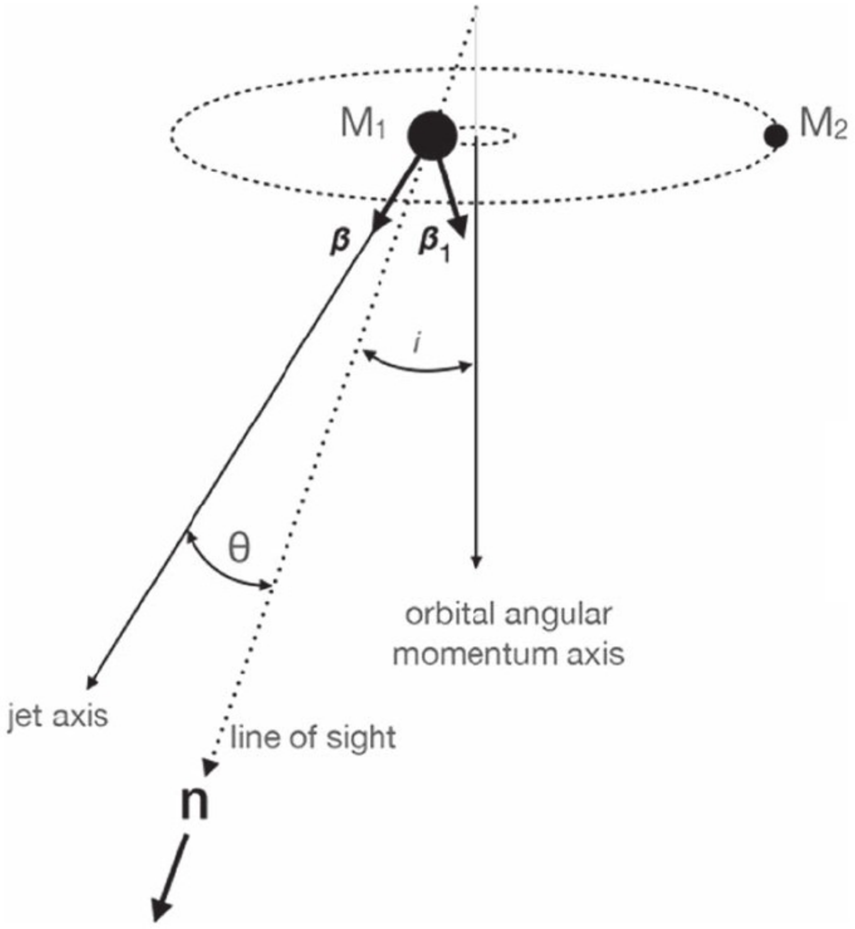

$$S = \mathcal{D}^{2-\alpha} S'$$

$$\delta \ln S = \frac{2(2-\alpha)\gamma^2\theta\beta_1\cos i}{(1+\gamma^2\theta^2)}\cos(2\pi t/P).$$

O'Neill+2022

Why is the periodicity turning on and off?

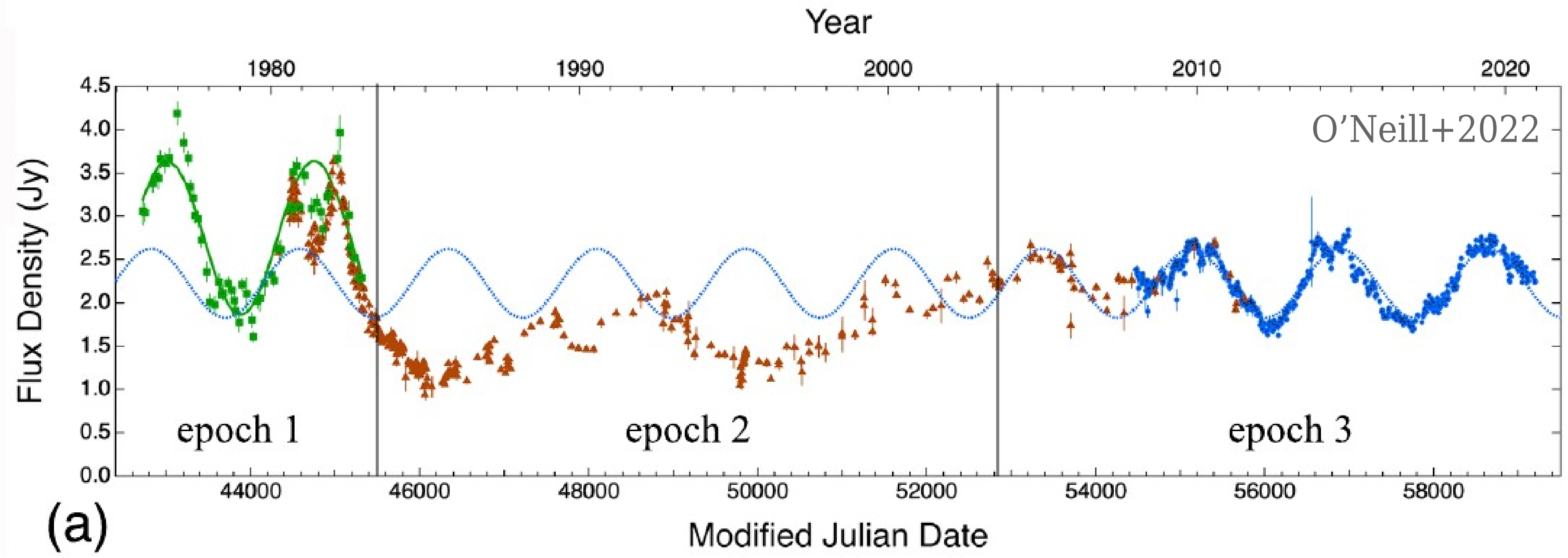

A unique super-massive black hole binary candidate

Binary separation and orbital period

$$r \sim 0.001 - 0.1\, pc \quad \text{for} \quad m \sim 3\times10^{6} M_{\odot} - 3\times10^{9} M_{\odot}$$

$$P_{rf} = 2\, yr$$

Implications for gravitational wave emission

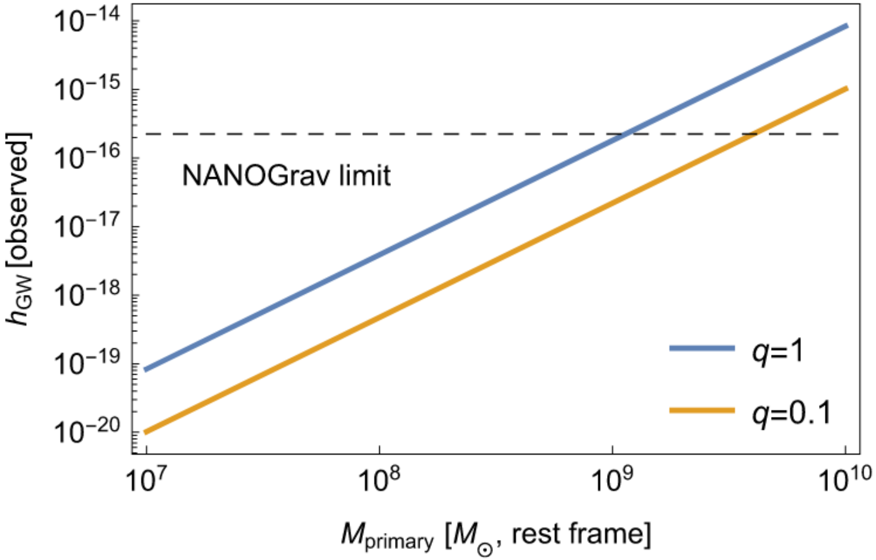

O'Neill+2022

The Astrophysical Journal Letters, 926:L35 (21pp), 2022 February 20 https://doi.org/10.3847/2041-8213/ac504b

The Unanticipated Phenomenology of the Blazar PKS 2131–021: A Unique Supermassive Black Hole Binary Candidate

S. O'Neill[1], S. Kiehlmann[2,3], A. C. S. Readhead[1,3], M. F. Aller[4], R. D. Blandford[5], I. Liodakis[6], M. L. Lister[7], P. Mróz[8], C. P. O'Dea[9], T. J. Pearson[1], V. Ravi[1], M. Vallisneri[10], K. A. Cleary[1], M. J. Graham[11], K. J. B. Grainge[12], M. W. Hodges[1], T. Hovatta[6,13], A. Lähteenmäki[13,14], J. W. Lamb[1], T. J. W. Lazio[10], W. Max-Moerbeck[15], V. Pavlidou[2,3], T. A. Prince[11], R. A. Reeves[16], M. Tornikoski[13], P. Vergara de la Parra[16], and J. A. Zensus[17]


S. O'Neill


S. Kiehlmann

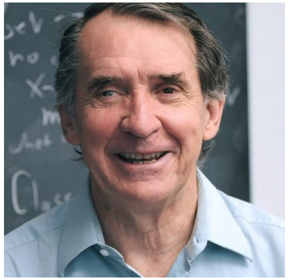
A.C.S. Readhead

Additional slides

WWZ transform: two epochs with matching period

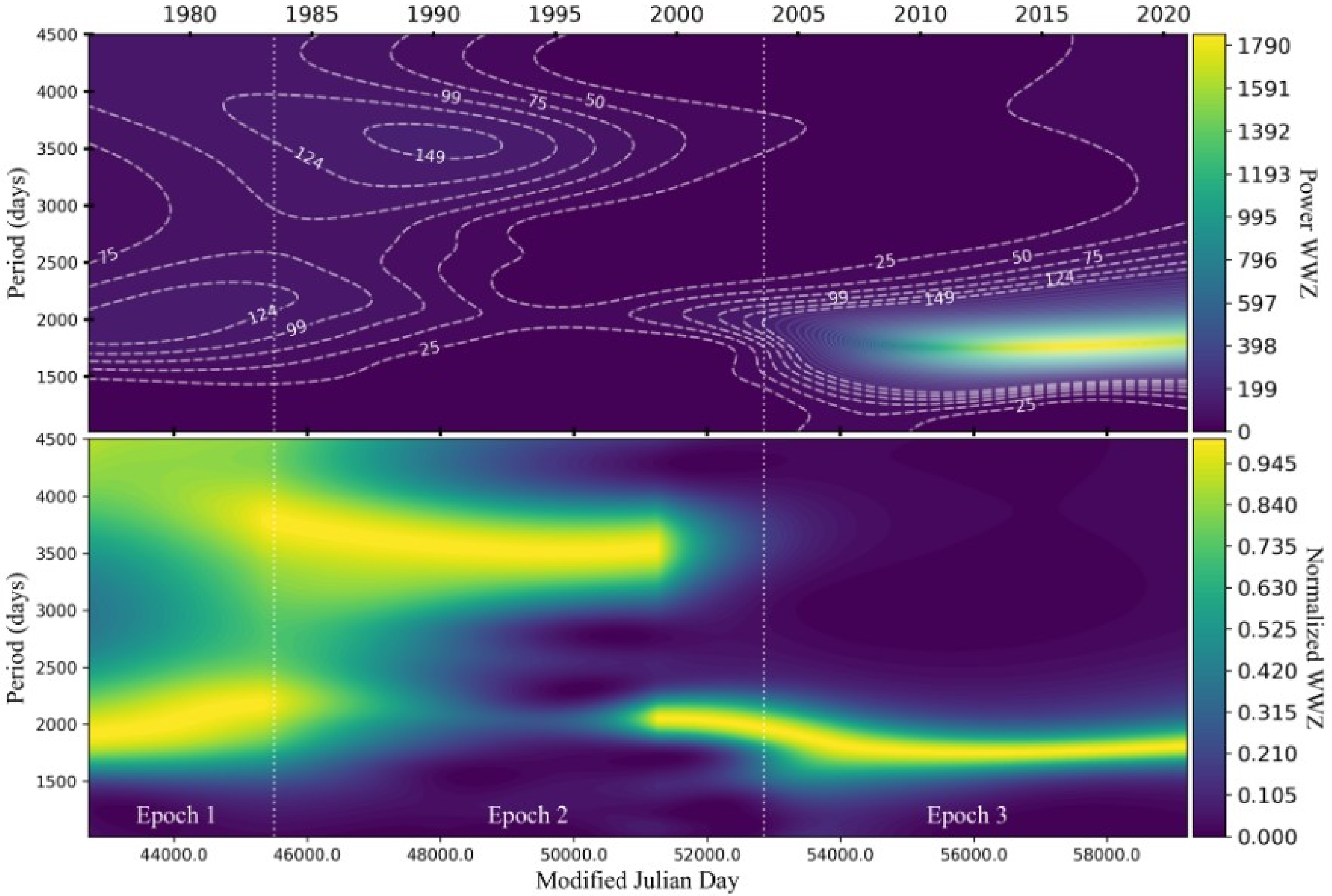

O'Neill+2022

Generalized Lomb-Scargle Periodogram: look-elsewhere

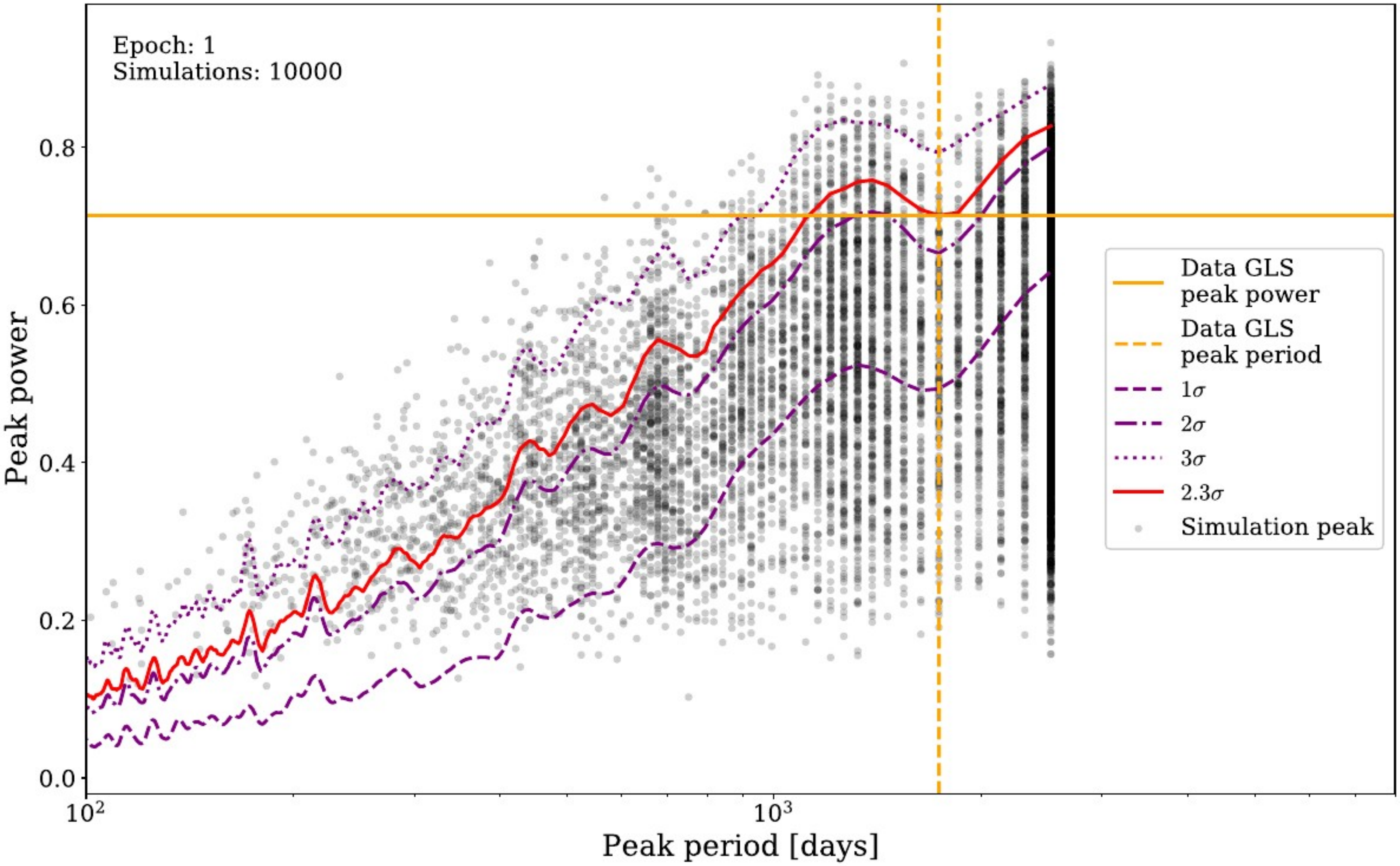

O'Neill+2022

Super Massive Black Hole Binary candidates

Source	Separation	Mass	Orbital period	References
B3 0402+379	7.3 pc (projected)	$1.5 \times 10^{10}\ M_\odot$	3×10^{4} yr	Rodriguez+ 2006, Bansal+ 2017
OJ 287	~0.1 pc	$1.8 \times 10^{10}\ M_\odot$ $1.5 \times 10^{8}\ M_\odot$	9 yr	Sillanpaa+ 1988, Valtonen+ 2016, Dey+ 2021